Imaging green fluorescent protein fusion proteins in *Saccharomyces cerevisiae*

Sidney L. Shaw, Elaine Yeh, Kerry Bloom and E.D. Salmon

Tagging expressed proteins with the green fluorescent protein (GFP) from *Aequorea victoria* [1] is a highly specific and sensitive technique for studying the intracellular dynamics of proteins and organelles. We have developed, as a probe, a fusion protein of the carboxyl terminus of dynein and GFP (dynein–GFP), which fluorescently labels the astral microtubules of the budding yeast *Saccharomyces cerevisiae*. This paper describes the modifications to our multimode microscope imaging system [2,3], the acquisition of three-dimensional (3-D) data sets and the computer processing methods we have developed to obtain time-lapse recordings of fluorescent astral microtubule dynamics and nuclear movements over the complete duration of the 90–120 minute yeast cell cycle. This required low excitation light intensity to prevent GFP photobleaching and phototoxicity, efficient light collection by the microscope optics, a cooled charge-coupled device (CCD) camera with high quantum efficiency, and image reconstruction from serial optical sections through the 6 μm-wide yeast cell to see most or all of the astral molecules. Methods are also described for combining fluorescent images of the microtubules labeled with dynein–GFP with high resolution differential interference contrast (DIC) images of nuclear and cellular morphology [4], and fluorescent images of the chromosomes stained with 4,6-diamidino-2-phenylindole (DAPI) [5].

Address: Department of Biology, University of North Carolina at Chapel Hill, Chapel Hill, North Carolina 27599-3280, USA.

Correspondence: E.D. Salmon
E-mail: tsalmon@email.unc.edu

Results and discussion

The imaging system

Our microscope [2,3] uses conventional wide-field optics and a cooled, slow-scan CCD camera for image detection (Figure 1). Many aspects of the microscope have been automated and are controlled by a Pentium-based computer system running MetaMorph software developed by Universal Imaging Corporation [2,3]. The Nikon FXA upright microscope has the advantage that the camera detector is placed at the primary focal plane of the objective lens, with
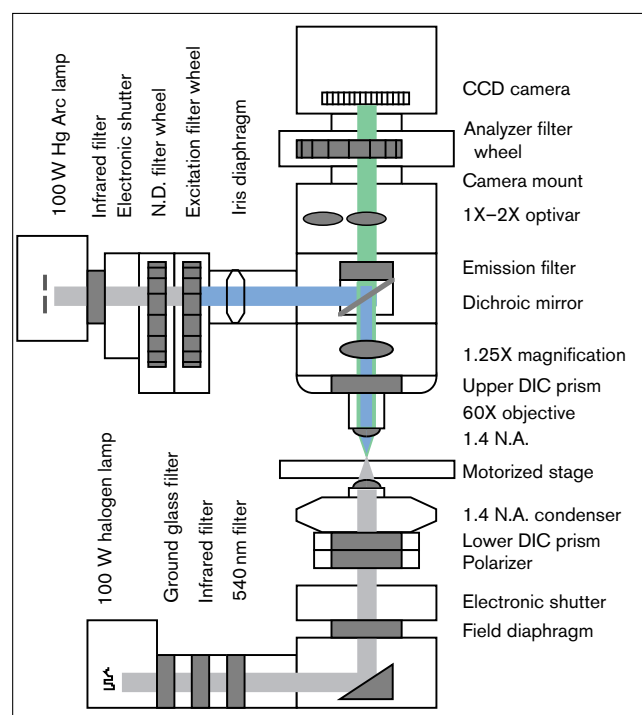
Multimode optical microscope. Modification of our original imaging system (for component list, see [2] or [3]) by the addition of a filter wheel containing the DIC analyzer allowed automated switching between DIC and fluorescent modes. Numerical aperture, N.A.; neutral density, N.D.

few intervening components to induce loss of light. For GFP imaging in yeast, we used a 60X, 1.4 numerical aperture (N.A.) objective lens, a 1.25X body tube lens and a 2X intermediate lens to project images to the camera at a total magnification of 150X. A 1.4 N.A. lens has a diffraction-limited lateral resolving power for 540 nm fluorescent light of about 235 nm, so that two barely resolvable points are separated on the camera detector by 150×235 nm (about 35 μm). Our CCD chip is composed of pixel element detectors that are 12 μm in size. Having 3 pixels per resolved unit satisfies the sampling criteria (Nyquist limit) for insuring that we are accurately sampling all of the resolvable information for high resolution DIC images [6,7]. The TC-215 CCD chip in the camera has a 35% chance of converting a 'green' photon to an electron (0.35 quantum efficiency). Therefore, of the 30% of the photons that our imaging system collects, 35% of those photons are converted to electrons stored in the CCD wells. This brings the total efficiency of our imaging system to about 10%. In order to gain sensitivity for our fluorescent images, we binned (grouped)

the pixels two-by-two on the chip during read-out, giving a pixel size of 24 μm. By binning the wells in the CCD chip, we sacrificed half of the spatial resolution in fluorescence for a four-fold increase in light sensitivity.

Filter wheels and shutters controlled light intensity for both DIC and fluorescence illumination pathways. The microscope was aligned for high resolution DIC microscopy as described by Yeh *et al.* [4]. In DIC microscopy, polarized light used to illuminate the specimen must pass through a second polarizing filter before reaching the camera. The second polarizing filter, termed an analyzer, typically has less than 30% transmission efficiency and would block the light from fluorescent emission if left in the light path. To circumvent this problem, the analyzer was rotated into the light path for DIC imaging — using a computer-controlled filter wheel (Ludl Biopoint 99B100) in front of the camera — and rotated out for fluorescent images; a glass blank was moved into the light path to match the focal shift of the analyzer. A custom camera mount was created to replace the C-mount camera adapter from the Nikon FXA, such that the CCD camera still resides at the primary focal plane of the objective lens and remains parfocal with the microscope oculars.

For fluorescent excitation, we used a multiple band-pass dichromatic mirror in combination with an excitation filter wheel to rapidly switch between GFP and DAPI imaging [2]. Using this optical method, the green and blue fluorescent images were always aligned on the CCD detector. A 490 ± 10 nm wavelength band-pass filter was selected for GFP excitation and a 360 ± 20 nm wavelength filter was selected to excite DAPI. A neutral-density filter of optical density 1 was used in combination with a manual iris diaphragm to attenuate the light from the 100 W Hg arc lamp to between 1% and 10% of maximum. The multiple band-pass filter cube (Chroma 83000 series) had a dichromatic beamsplitter (505–510 nm) and emission band-pass filter (515–550 nm) broad enough to include the emission from GFP containing a Ser65→Thr amino acid substitution [1]. In addition, the same filter cube allowed passage of blue light from DAPI (400 nm dichroic, 460 ± 50 nm band-pass). The dichromatic mirror and emission filter were of high transmission efficiency and compare favorably with other filters produced specifically for GFP, such as the 'Hi-Q' and 'Endow' filter cubes (Chroma).

Image acquisition

For high resolution imaging, the yeast cells were immobilized on the coverslip by mounting them in a thin layer of 25% gelatin (Sigma, Type A: G-2500) made with yeast medium as described by Yeh *et al.* [4]. The gelatin also substantially enhances the quality of DIC images by reducing the refractive index mismatch between the cell wall and the aqueous medium ([4], a method originally suggested by Tim Stearns).
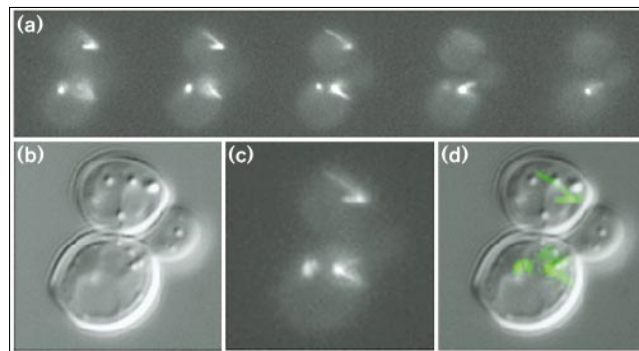
Astral microtubules labeled with dynein–GFP in a yeast cell. **(a)** Five images at 1 μm intervals through the cell show the majority of GFP fusion protein present. **(b)** The corresponding DIC image for the middle GFP image in (a). **(c)** Projection of the five image planes in (a) onto a single image plane as depicted in Figure 3c. **(d)** A color overlay of the images in (b) and (c). To obtain these images and those in Figure 4, we constructed a plasmid encoding dynein–GFP under the control of the galactose-inducible promoter Gal1. Cells were induced with galactose for only 2 h to prevent the negative effects of overexpression (S.L.S., E.Y., E.D.S. and K.B., unpublished observations).

For healthy cells displaying wild-type cell cycle times, the dynein–GFP fluorescence was very weak, barely detectable by the dark-adapted eye, and required a sensitive detector like the cooled CCD camera for achieving high quality images. This is because dynein–GFP must be expressed at very low levels to avoid stabilizing astral microtubule dynamics and blocking cell cycle progression (Figure 2 and S.L.S., E.Y., E.D.S. and K.B., unpublished observations). In addition, exposure of the cells to excitation light of a wavelength of 490 nm or less must be kept at a minimum to avoid GFP photobleaching and phototoxic effects on the cells (S.L.S., E.Y., E.D.S. and K.B., unpublished observations).

Taking exposures of a duration of 3 seconds with a two-by-two binning at 1–10% of maximum excitation light generated images of yeast astral microtubules labeled with dynein–GFP which had — in our camera, after subtraction of a 'dark-background' image — 50–250 gray levels above a random noise floor of 20–30 gray levels (Figures 2,3). An average dark-background image was obtained for each experiment by taking 25 camera exposures of 3 seconds with the camera shutter closed. Averaging these images yielded a single image representing the average accumulation of electrons in each pixel generated by thermal effects (thermal noise), and the gray-level counts contributed by the read-out amplifiers (read-out noise) [8,9]. This image also contained an exact copy of the pixel inhomogeneities, or 'hot pixels', which show up very brightly against the dark background. Dark-background image subtraction did not correct for the random variations in either thermal or read-out noise. Cooling the CCD chip to −40°C removed most of the random thermal noise for exposures of less than 5 seconds, and the root mean square

Figure 3
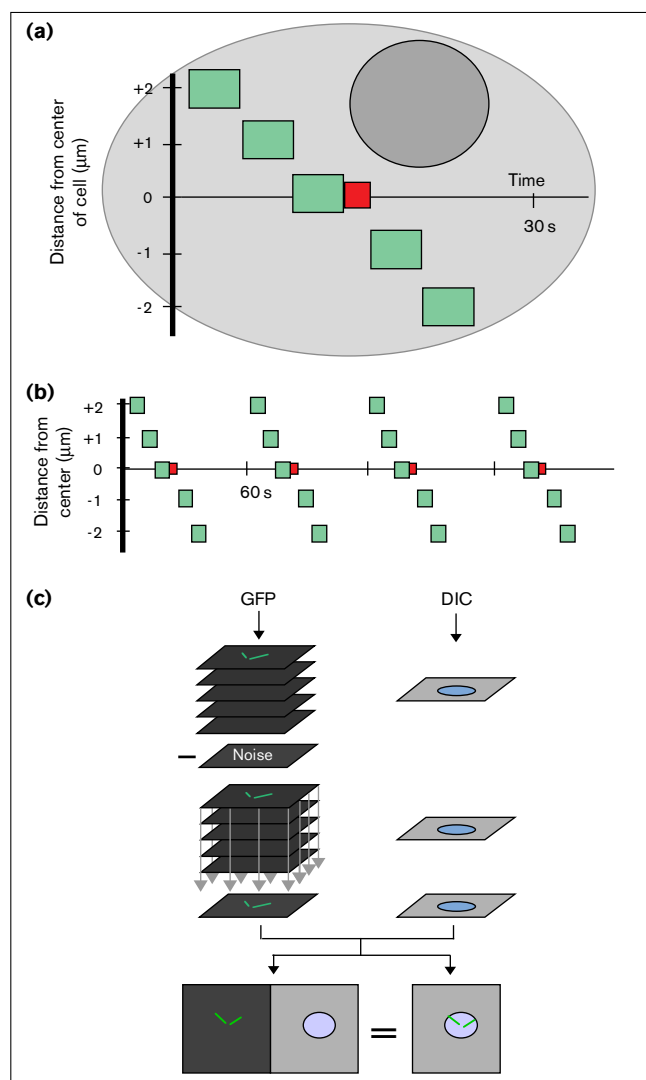
Image acquisition and processing. **(a)** Five fluorescent images (green) were taken at 1 μm intervals; a single DIC image (red) was taken in the same focal plane as the middle fluorescent image, as were any DAPI images. The stage was then returned to the original position with a slight adjustment to account for a hysteresis in the microscope focusing apparatus. **(b)** The acquisition regime was iterated every 60 s for time-lapsed imaging. **(c)** Image processing schematic. The background was subtracted from image stacks of raw fluorescent data, which were then projected as sets of five to a 2-D representation of the 3-D data set. DIC and GFP images were overlaid after adjusting for a spatial offset in horizontal and vertical directions. Details are described in Materials and methods.

read-out noise was about 10 electrons, or 2 gray levels after digitization, for our camera. After dark-background image subtraction, the major noise components in the image were autofluorescence from the cell and media and the photon counting noise (which depends on the root mean square or standard deviation of the number of photons captured in an exposure). A signal-to-noise ratio of between 1.5:1 and 5:1 produced an acceptable image of microtubules. Cells grew with wild-type kinetics at these

low levels of fluorescent excitation, even though imaging was eventually limited by the GFP photobleaching produced by 500–1000 exposures of 3 seconds.

We found that for a 5–8 μm-wide yeast cell, we could not determine the position of the astral microtubules from a single optical section (Figure 2). Figure 3 depicts the image acquisition and processing routines we used to acquire a 3-D data set. A computer controlled stepping motor attached to the fine focus control (Figure 1) was used to automatically acquire the five dynein–GFP images along the Z-axis at 1 μm intervals (Figure 3a). A single 600 millisecond DIC exposure, corresponding to the central fluorescent image, was taken with each series of fluorescent images. To take the images in as short a time span as possible, we selected only the central 300×300 pixel area of the 1000×1000 pixel CCD chip for read-out. Image acquisition took 3 seconds for each fluorescent exposure and 1 second to read out the image and change the focal plane. The total time of execution for the acquisition protocol was around 23 seconds. This image acquisition process was repeated once every 60 seconds (Figure 3b).

When required, a single 3 second exposure of the DAPI-labeled nucleus was taken immediately following the DIC exposure in the acquisition protocol (Figure 4). We do not routinely image DAPI-stained preparations because cells imaged with DAPI stop growing within 45 minutes of imaging and our studies have required imaging of cell cycles of 90–120 minutes in duration.

Image processing
Once the images were captured and saved to computer memory (Figure 3a,b), the next task was to prepare the images for analysis and presentation (Figure 3c). The goal for processing the fluorescent data was to remove noise from the images, to present the information from the five Z-axis planes in a single image, and to overlay that information onto the corresponding DIC image (Figure 3c and Materials and methods). Digital deconvolution [10,11] of the five image planes to produce a sharpened image was not required to understand the position of microtubules in the cell. In order to test the alignment of our processed fluorescent images with DIC images we used 1 μm fluorescent beads; we determined that when we overlaid the resultant images from our fluorescent and DIC exposures, the DIC image was shifted 6 pixels in the horizontal dimension and 3 pixels in the vertical dimension. We therefore adjusted for this shift when overlaying our images (Figure 3c) and for all subsequent measurements. The resulting image overlay of the yeast cells, when the fluorescence from dynein–GFP was included, gave a 2-D representation of the entire population of astral microtubules localized to the nucleus (Figures 2,4; the nucleus is observed in the DIC image).

Figure 4
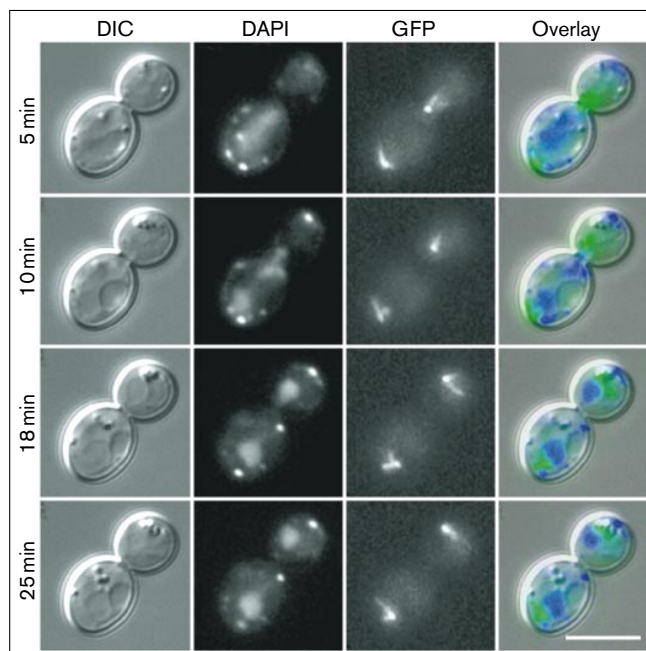
Multimode time-lapse imaging of spindle elongation and nuclear division in budding yeast. The cells were prepared for microscopy as described in the legend to Figure 2. Labeling of nuclei with DAPI [5] was performed by adding 5 µl of 1 mg ml^{-1} DAPI in DMSO to a 1 ml logarithmic phase culture for 30 min. The DAPI-containing medium was exchanged for fresh medium before imaging. Four sets of images were selected from a time-lapse series showing DIC, DAPI, GFP and overlayed images (as indicated) of the same specimen at the indicated time after the onset of anaphase. The multimode images reveal that the transition from a sausage-shaped nucleus to a bi-lobed shape, previously observed using DIC [4], is accompanied by the separation of the chromatin, observed using the DNA-intercalating dye, DAPI. The bar is 5 µm.

Putting images into motion

The dynein–GFP fusion protein has allowed us to visualize the dynamic behavior of the microtubule cytoskeleton and the spindle poles (S.L.S., E.Y., E.D.S. and K.B., unpublished observations). Though the single images of astral microtubules and the nucleus look very similar to images obtained from fixed cells immunostained using anti-tubulin antibodies and stained with DAPI, putting the multimode images into motion provides critical new information. Playing the time-lapsed overlay, we can observe the dynamics of the microtubules with reference to the nucleus and the growing bud (Figures 2,4). Quicktime movies of image series prepared in this manner may be accessed via the world wide web at http://www.unc.edu/depts/biology/bloomlab/gfp.htm.

Materials and methods

Image storage
We store image data either to a 3 gigabyte internal hard disk or to a removable 1 gigabyte Jaz (Iomega) cartridge. The data are eventually written to a 650 megabyte compact disk for permanent archival. The raw data for each experiment consisted of two files, each containing a series of either DIC or fluorescent images. There are five 150×150 pixel GFP images for every one 300×300 pixel DIC image. For a typical time-lapse experiment that acquires an image set every minute for 75 min, 13.2 megabytes are required for the DIC file and 16.5 megabytes for the GFP file. Due to the large file sizes and computationally intensive image processing, we run our PC-based software on a 200 MHz Pentium chip computer system with 128 megabytes of RAM.

Processing 3-D data sets
The averaged dark image was subtracted from each of the GFP fluorescent images, leaving only the signal from the specimen and the random noise component of the dark current and read-out. The five Z-axis images were converted to a single composite image by using the brightest pixel at every position in each of the five image planes (Figure 3c). This maximum pixel projection technique produced a 2-D representation of the GFP fusion proteins within the cell from the 3-D data set. A macro created with the MetaMorph scripting language was used to input the entire stack of background-subtracted images and output a new stack of only the projected images. To compensate for GFP photobleaching, the gray level of each image in the new stack was multiplied by a scaling factor computed from the average value of the signal in the first image. Finally, the 150×150 pixel images were spatially scaled using a bicubic interpolation to 300×300 pixels so that they could be overlaid onto the DIC images.

Multimode image overlays
To begin construction of a multimode image overlay, the images were converted from 12 bits (4096 gray levels) to 8 bits (256 gray levels). Our software generates color using three 8 bit images, representing red, green and blue, combined to yield a final 24 bit color image. As the majority of our 12 bit GFP images contain only 50–250 useful gray levels, conversion does not compromise the intrascenic dynamic range. The previously calculated offset of the two images required that we crop the GFP image displaced from the DIC image before making the overlay. The creation of an overlay was facilitated by the implementation of a routine within our software package that converts the DIC image to RGB grayscale, in which each R, G, and B value is equal, and false-colors the 8 bit GFP image. The brightness of either image was changed corresponding to a percentage scale selected by the user. The GFP image was subtracted from the DIC image such that the apparent intensities of the two images could be kept comparable when the 'green' GFP image was then added to the DIC image.

References

1. Heim R, Chen RY: **Engineering green fluorescent protein for improved brightness, longer wavelengths and fluorescence resonance energy transfer.** *Curr Biol* 1996, **6:**178-182.
2. Salmon ED, Inoue T, Desai A, Murray AW: **High resolution multimode digital imaging system for mitosis studies *in vivo* and *in vitro*.** *Biol Bull* 1994, **187:**231.
3. Salmon ED, Waters JC: **A high resolution multimode digital imaging system for fluorescence studies of mitosis.** In *Analytical Use of Fluorescent Probes in Oncology.* Edited by Kohen and Hirschberg. New York: Plenum Press; 1996.
4. Yeh E, Skibbens R, Cheng J, Salmon ED, Bloom KS: **Spindle dynamics and cell cycle regulation of dynein in the budding yeast, *Saccharomyces cerevisiae*.** *J Cell Biol* 1995, **130:**687-699.
5. Palmer RE, Koval M, Koshland D: **The dynamics of chromosome movement in the budding yeast *Saccharomyces cerevisiae*.** *J Cell Biol* 1995, **130:**687-699.
6. Inoue S, Spring K: *Video Microscopy: The Fundamentals*, 2nd edn. New York: Plenum Press; 1997.
7. Salmon T, Walker RA, Pryer NK: **Video-enhanced differential interference contrast light microscopy.** *Biotechniques* 1989, **7:**624-633.
8. Aikens RS, Agard D, Sedat JW: **Solid state imagers for microscopy.** *Methods Cell Biol* 1989, **29:**292-313.
9. Farkas DL, Gough AH, Lanni F, Taylor DL: **A guide to selecting electronic cameras for light microscopy-based imaging.** *Am Laboratory* 1995, **27:**25-40.
10. Hiroka Y, Swedlow JR, Paddy MR, Agard D, Sedat JW: **Three-dimensional multiple-wavelength fluorescence microscopy for the structural analysis of biological phenomena.** *Semin Cell Biol* 1991, **2:**153-165.
11. Carrington WA, Lynch RM, Moore EDW, Isenberg G, Forarty KE, Fay FS: **Supperresolution three-dimensional images of fluorescence in cells with minimal light exposure.** *Science* 1995, **268:**1483-1487.